Journal of Geography and Geology; Vol. 10, No. 4; 2018
ISSN 1916-9779 E-ISSN 1916-9787
Published by Canadian Center of Science and Education

Fractal-Based Computation of Heat Source Depths and Temperatures for the Soutpansberg Basin, South Africa

Peter K. Nyabeze[1] & Oswald Gwavava[1]

[1] Department of Geology, University of Fort Hare, Alice, South Africa

Correspondence: Peter Nyabeze, Department of Geology, University of Fort Hare, Alice, EC., 5700, South Africa. E-mail: 201013945@ufh.ac.za

Received: August 3, 2018 Accepted: September 10, 2018 Online Published: November 16, 2018

doi:10.5539/jgg.v10n4p10 URL: http://dx.doi.org/10.5539/jgg.v10n4p10

Abstract

The fractal-based approach was used for computing magnetic depths and temperatures for the Soutpansberg Basin in South Africa. The average depth to the top Z_t and basement depth Z_o for the Soutpansberg Basin were 4.36 ± 0.28 km, 10.43 ± 0.65 km, respectively. The average temperature at depth Z_t was 184.69 ± 7.66 ºC. Magnetic source depths and basal temperatures that were in the Curie point range were determined, to be within 20.35 km to 21.68 km and 549.34 ºC to 585.24 ºC, respectively. Increasing the value of the fractal parameter β from 0 to 4, had an effect of retaining deeper depths and higher temperatures. The fractal parameter values of $\beta > 3$ retained Curie point depths and temperatures that indicated basal rock types with an igneous predisposition. The fractal-based approach proved to be an improved technique as compared to the conventional centroid method.

Keywords: depth, fractal parameter, geothermal potential, hot spring, power spectra

1. Introduction

Depths and temperatures of magnetic sources were computed for the Soutpansberg Basin in northern part of South Africa, from power spectra of the airborne magnetic data from square data blocks with sides with dimensions *L* of 51 km, 103 km, and 129 km (Figure 1). Ledwaba *et al.* (2009) reported that the airborne magnetic data for the study area was collected in 1973 along survey lines that were 1000 m apart, maintaining a mean sensor elevation of 150 m. The aim of the research was to characterise the heat sources and investigate the geothermal potential of the Soutpansberg Basin. Jones (2017) reported that the formation heat for the northern part of South Africa was due to radiogenic elements such as uranium, thorium or potassium. Jones (2017) attributed the anomalous heat flow in the study area, to the concentration of geothermal heat by the deep-seated circulation of meteoric water.

The conventional computation of magnetic source depths from the analysis of Fourier Transform computed spectra data was reported to result in the overestimation of Curie Point Depth in studies by Bansal *et al.* (2016) and Khojamli *et al.* (2017). Bansal *et al.* (2016) mentioned that conventional methods assumed that magnetic sources had distribution that were random and uncorrelated, and further stated that the sources follow random and fractal distributions. Nyabeze & Gwavava (2016) used the conventional centroid and spectral peak methods and achieved basal depths and temperature that were below the Curie point values for the Soutpansberg Basin. Nwankwo *et al.* (2009) defined the Curie point as having a temperature of 580 °C.

Pilkington and Todoeschuck (1993) reported that the magnetic sources displayed random and fractal distributions. Bansal *et al.* (2016) however reported that the simultaneous estimation of depth and scaling exponents was a limitation of the fractal-based approach for computing depth. The correction of the power spectrum before computing the depth to the top of magnetic sources using magnetic data was reported by Bouligand *et al.* (2009) and Salem *et al.* (2014).

Bansal *et al.* (2011) corrected the power spectrum for scaling distribution of magnetic sources for the computation of both depth to the top Z_t and the centroid Z_o. Khojamli *et al.* (2017) and Ravat *et al.* (2007) stated that fractal source distributions had power spectra proportional to $k^{-\beta}$, where k represented the wavenumber and β denoted the fractal parameter. Values of β where reported to be varying between 1.5 to 5.8 for lithology types ranging from sedimentary to igneous (Khojamli *et al.*, 2017). The value of β was found to be equal to 4 for data from South Africa by Maus *et al.* (1997). Ravat *et al*. (2007) stated that the power spectrum for random depth source variations was associated with a β value of 2.9. Akbar & Fathianpour (2016) applied the Fractal Based Approach and computed depths for blocks with dimensions of L of 10 km and 51 km for the Sabalan geothermal field in Iran, and obtained depths in the 5.2 km range, that were closer to the actual well depth and comparable to those obtained using an L of 100 km.

Bektas *et al.* (2007) mentioned that the Curie Temperature for magnetite was 580 °C and that the Curie Point depth was determined from the temperature versus depth graph. Curie Point values were reported as being 573 °C for quartz, 585 °C for magnetite, 770 °C for iron, and that values for the upper lithosphere varied between 550 °C and 580°C (Arnaiz-Rodriguez & Orihuela, 2013). Temperatures below the maximum depth of magnetic source of approximately 40 km should be above the Curie point value of approximately 550 °C (Telford *et al.*, 1990). Campbell *et al.* (2016) reported the existence of sedimentary basins in the south and south-eastern part of South Africa with temperatures ranges above 200°C to 230°C at depths below 1 km to 3.5 km.

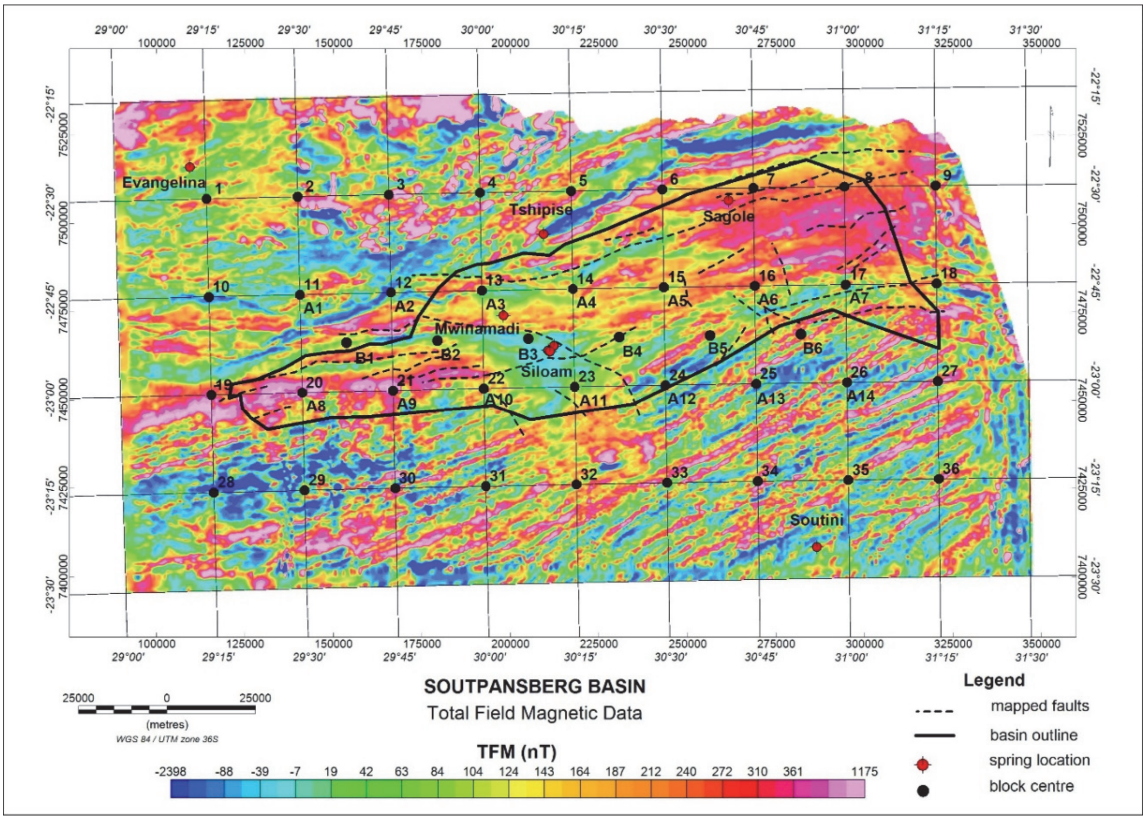

Figure 1. Total field magnetic data showing the outline of the Soutpansberg Basin, hot springs as red symbols, block centres 1-36, A1-A14, and B1-B6 for blocks with dimensions L of 51 km, 103 km and 129 km, respectively and mapped geological faults (after Barker *et al.,* 2006).

2. Method

Airborne data window sizes with L dimensions of 51 km, 103 km, and 129 km were utilised for spectral analyses of data for depth determinations. The number of data magnetic blocks with L dimensions of 51 km, 103 km, and 129 km were 36, 14, and 6 respectively. The largest window size with L of 129 km was chosen to ensure the preservation of spectral signatures. The computation of depth to the top Z_t and depth to the centroid Z_o, after Bansal *et al*. (2016) and Khojamli *et al.* (2017), involved the correction of power spectrum for the distribution of sources and obtained the following relationships, as Equation 1:

$$\ln\left(k^{\beta}\left(P(k)\right)\right) = A_2 - 2kZ_t, \tag{1}$$

and the depth to the centroid Z_o is obtained, as Equation 2:

$$\text{In}\ \left(k^{\beta}\left(\frac{\rho(k)}{k^2}\right)\right) = A_3\text{-}2\,kZ_0 \tag{2}$$

where k is the wavenumber, β is the scaling component, and $k^{-\beta}$ being a scaling factor.

The basal depth, Z_b is computed using Equation 3 below,

$$Z_b = 2Z_o - Z_t \quad (3)$$

where Z_o is the depth to the centroid, and Z_t is the depth to the top of a geological body (Ravat *et al.,* 2007; Eletta and Udensi, 2012). The Curie temperature T_c is computed, as in Equation 4:

$$T_c = [\frac{dT}{dZ}]\, Zc \quad (4)$$

where, Θ_c is the Curie temperature and dT/dZ is the geothermal gradient and Z_c is the Curie depth (Kasidi and Nur, 2013). The depth to the top Z_t was determined from the gradient $2Z_t$ of the graph of spectral energy versus wavenumber k (km^{-1}) for wavelength between 0.50 and 0.20 (km^{-1}). The depth to the basement or centroid Z_o was determined from the gradient $2Z_o$ of the graph of spectral energy versus the wavenumber k for wavelength between 0.10 and 0.5 (km^{-1}). The depth to the basal Z_b and corresponding Curie point depths were computed using depths Z_t and Z_o. All depths and basal temperatures were computed by applying fractal parameter values of β ranging between 0 to 4.

The subsurface formation temperature T_f is calculated, as in Equation 5:

$$T_f = T_s + G_t Z\,, \quad (5)$$

where T_f is the temperature at depth, T_s is the temperature at the surface, G_t is the geothermal gradient and Z is the source depth (Tiab & Donaldson, 2015). The geothermal gradient, G_t for the study area was 27 °C/km (Jones, 1992) and an average temperature of water at the hot spring T_s was 67.5 °C (Brandl *et al.,* 2001 and Shabalala *et al*., 2015).

3. Results

The Fractal based approach for depths Z_t, Z_o and Z_b and corresponding formation temperatures T_t, T_o and T_b for L values of 51 km, 103 km and 129 km for fractal parameters β = 0 to 4, are presented in Table 1, Table 2 and Table 4, respectively. Results showed wider standard deviations from the mean for data obtained using different fractal parameter values β of 0 to 4. The standard deviation for depths Z_t, Z_o and Z_b were 14.00% to 15.50%, 27.10% to 27.70% and 30.40% to 31.04%, respectively.

Depths and temperatures were computed for data points, N of 36, 14 and 6 for magnetic blocks with dimensions L of the of 51 km, 103 km and 129 km, respectively. Table 1 has standard deviations of the mean showing the comparison of results obtained from the application of the fractal parameter β on spectral data with specific data points N and window size L. The variation of mean depth and temperature results were 0.6% to 6.6% and 0.5% to 6.6%, respectively (Table 4). Table 5 has a comparison of depths and temperatures obtained for blocks with L values of 51 km, 103 km and 129 km, respectively with standard deviations between 6.20% and 6.50%.

The depths to the top Z_t, for L dimensions of 51 km and 103 for β = 3, are in the range 4.70 km to 4.80 km (Figure 2) and 4.40 km to 4.60 km (Figure 3), respectively. Figure 4 has an illustration of the depth to the top Z_t, basement depth Z_o and basal depth Z_b for blocks with L= 129 km fractal from application of fractal parameter β = 3 showing depths in the range 5.20 km to 5.37 km, 13.26 km to 13.50 km and 21.24 km to 21.67 km, respectively.

Table 1. Depth to the top Z_t, basement depth Z_o, basal depth Z_b and corresponding formation temperatures T_t, T_o and T_b for fractal parameters 0 to 4 for L= 51 km

L (km)	β	Z_t *(km)*	Z_o *(km)*	Z_b *(km)*	T_t *(ºC)*	T_o *(ºC)*	T_b*(ºC)*
51	0	3.35	6.36	9.36	157.46	238.65	252.83
51	1	3.80	8.41	13.02	169.49	294.08	351.67
51	2	4.24	10.46	16.69	181.53	349.51	450.50
51	3	4.69	12.52	20.35	193.56	404.95	549.34
51	4	5.13	14.57	24.01	205.59	460.38	648.17
Average		4.24	10.46	16.69	181.53	349.51	450.50
Std.Dev		0.63	2.90	5.18	19.03	87.65	139.77
Std.Dev (%)		14.8%	27.70%	31.04%	10.48%	25.08%	31.04%

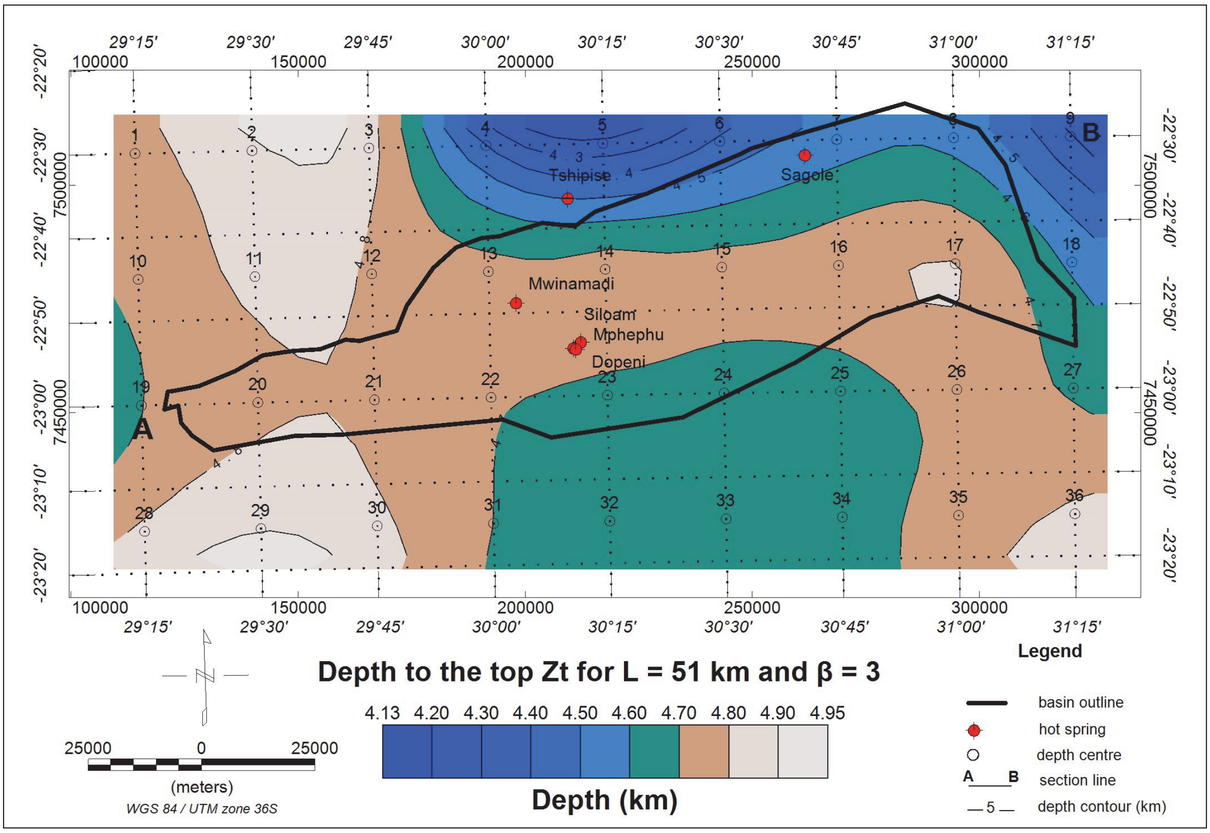

Figure 2. Depth to the top Z_t, for fractal parameters $\beta = 3$, for L= 51 km, showing an east to west feature in the central part of the basin with hot springs, at a depth range of 4.70 km to 4.80 km

Table 2. Depth to the top Z_t, basement depth Z_o, basal depth Z_b and corresponding formation temperatures T_t, T_o and T_b for fractal parameters 0 to 4 for *L*= 103 km

L (km)	*β*	*Zt (km)*	Z_o *(km)*	Z_b *(km)*	T_t *(ºC)*	T_o *(ºC)*	T_b*(ºC)*
103	0	3.22	5.93	8.64	154.01	227.08	233.16
103	1	3.65	7.77	11.90	165.65	276.92	321.18
103	2	4.09	9.62	15.16	177.3	326.75	409.20
103	3	4.52	11.47	18.42	188.94	376.58	497.22
103	4	4.95	13.31	21.68	200.58	426.41	585.24
Average		4.09	9.62	15.16	177.30	326.75	409.20
Std.Dev		0.61	2.61	4.61	18.41	78.79	124.48
Std.Dev (%)		15.00%	27.10%	30.40%	10.38%	24.11%	30.40%

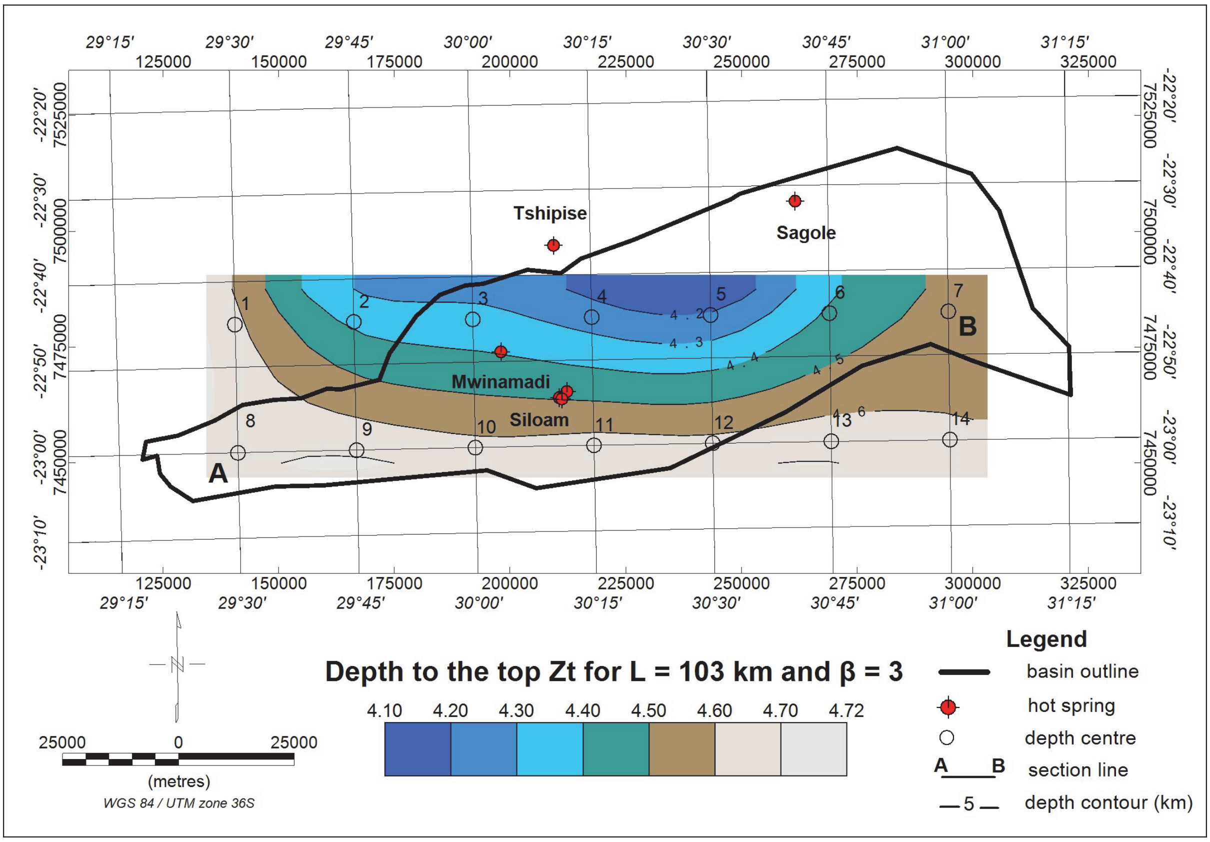

Figure 3. Depth to the top Z_t, for fractal parameters $\beta = 3$, for L= 103 km, showing a feature in the central part of the basin with hot springs, at a depth range of 4.40 km to 4.60 km

Table 3. Depth to the top Z_t, basement depth Z_o, basal depth Z_b and corresponding formation temperatures T_t, T_o and T_b for fractal parameters 0 to 4 for L= 129 km

L (km)	β	Z_t *(km)*	Z_o *(km)*	Z_b *(km)*	T_t *(ºC)*	T_o *(ºC*	T_b*(ºC)*
129	0	3.71	6.87	10.03	167.09	252.38	270.68
129	1	4.23	9.04	13.85	181.17	311.07	373.96
129	2	4.75	11.21	17.68	195.25	369.75	477.25
129	3	5.27	13.39	21.50	209.33	428.43	580.53
129	4	5.79	15.56	25.33	223.41	487.11	683.81
Average		4.75	11.21	17.68	195.25	369.75	477.25
Std.Dev		0.74	3.07	5.41	22.26	92.78	146.06
Std.Dev (%)		15.50%	27.40%	30.60%	11.40%	25.09%	30.60%

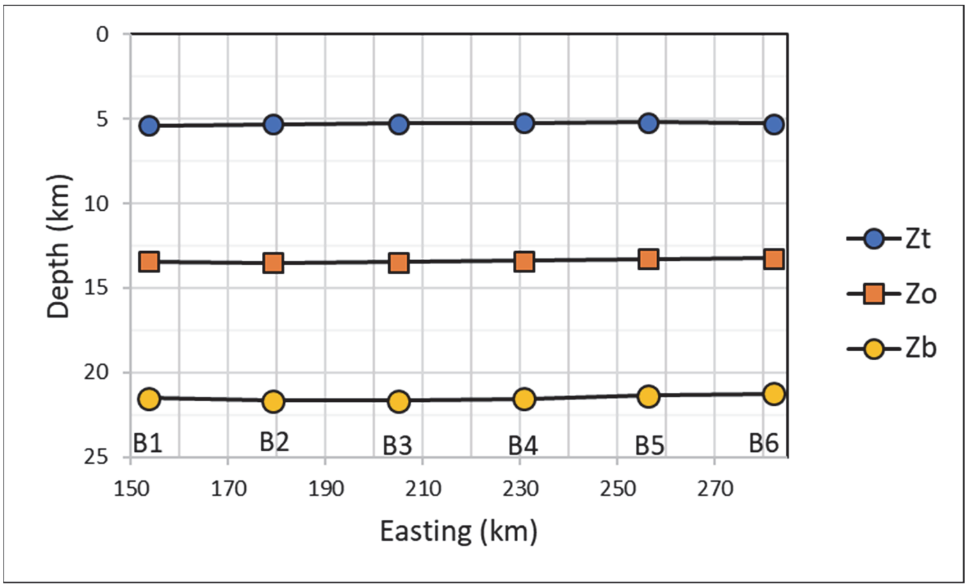

Figure 4. Depth to the top Z_t, basement depth Z_o and basal depth Z_b for fractal parameters $\beta = 3$, block size L= 129 km for data points B1 to B6

Table 4. Standard deviations of the mean for depth to the top Z_t, basement depth Z_o, basal depth Z_b and corresponding formation temperatures basal temperature T_t, T_o and T_b

L (km)	β	*N*	$\pm Z_t$ *(km)*	$\pm Z_o$ *(km)*	$\pm Z_b$ *(km)*	$\pm T_t$ *(ºC)*	$\pm T_o$ *(ºC)*	$\pm T_{b(ºC)}$
51	0	36	4.5%	4.6%	6.6%	2.6%	3.3%	6.6%
51	1	36	4.0%	3.5%	4.7%	2.4%	2.7%	4.7%
51	2	36	3.6%	2.8%	3.7%	2.3%	2.2%	3.7%
51	3	36	3.2%	2.3%	3.0%	2.1%	1.9%	3.0%
51	4	36	3.0%	2.0%	2.6%	2.0%	1.7%	2.6%
103	0	14	4.9%	2.8%	5.1%	2.8%	1.9%	5.1%
103	1	14	4.4%	2.1%	3.7%	2.6%	1.6%	3.7%
103	2	14	3.9%	1.7%	2.9%	2.4%	1.3%	2.9%
103	3	14	3.5%	1.4%	2.4%	2.3%	1.2%	2.4%
103	4	14	3.2%	1.2%	2.0%	2.1%	1.0%	2.0%
129	0	6	1.5%	1.3%	1.6%	0.9%	1.0%	1.6%
129	1	6	1.4%	1.0%	1.2%	0.9%	0.8%	1.2%
129	2	6	1.2%	0.8%	0.9%	0.8%	0.7%	0.9%
129	3	6	1.1%	0.7%	0.7%	0.7%	0.6%	0.7%
129	4	6	1.0%	0.6%	0.6%	0.7%	0.5%	0.6%
Max.			1.0%	0.6%	0.6%	0.7%	0.5%	0.6%
Min.			4.9%	4.6%	6.6%	2.8%	3.3%	6.6%

Table 5. Mean depths to the top Z_t, basement depth Z_o, basal depth Z_b and corresponding basal temperature T_b for blocks with L of 51 km, 103 km and 129 km

L (km	*N*	Z_t *(km)*	Z_o *(km)*	Z_b *(km)*	T_t *(ºC)*	T_o *(ºC)*	T_b (ºC)
51	36	4.24	10.46	16.69	181.53	349.51	450.50
103	14	4.09	9.62	15.16	177.30	326.75	409.20
129	6	4.75	11.21	17.68	195.25	369.75	477.25
Average		4.36	10.43	16.51	184.69	348.67	445.65
Std.Dev		0.28	0.65	1.04	7.66	17.56	27.99
Std.Dev (%)		6.48%	6.23%	6.28%	4.15%	5.04%	6.28%

4. Discussion

The value of computed depths and temperature increased with the application of higher fractal parameters values of β from 0 to 4 for blocks with L = 51 km, 103 km and 129 km. Depths Z_t, Z_o, and Z_b and basal temperatures were consistent within a unique value of β, with the low standard deviations below 1.2%. The variation of the average depths and temperature values for the three block sizes was below 6.5%, indicating that any block size with an appropriate fractal parameter can be used compute the source depth and temperature. A comparison of depths and temperatures for a fractal parameter range of β = 0 to 4, retained a large standard deviation between 14.80% to 31.04%, showing that changing β values influences depths and temperatures. The correction of depths using the fractal parameter was reported by Bansal *et al.* (2011), Bouligand *et al.* (2009), and Salem *et al.* (2014). Obtaining of different depths and temperatures for unique values of β was reported to be due to different types of lithologies (Khojamli *et al.*, 2015). The results showed that there was an improvement in the standard deviation of the mean for depths and temperature L = 51 km to L = 129 km. The Fractal based approach retained basal depths and corresponding temperatures that were within the Curie point range (Nwankwo *et al.*, 2009) for fractal parameter values of $\beta > 3$.

5. Conclusion

The average depth to the top Z_t and basement depth Z_o for the Soutpansberg Basin were 4.36 ± 0.28 km, 10.43 ± 0.65 km, respectively. The shallower depth to the top Z_t is important for geothermal exploration. The average temperature at depth Z_t was 184.69 ± 7.66 ºC, indicating geothermal potential. The application of a higher fractal parameters $\beta > 3$ achieved basal depths and temperatures within the Curie point range of 20.35 km to 21.68 km and 549.34 ºC to 585.24 ºC, respectively. The Curie depth at which basement rocks lost their magnetisation due to heat, the Curie Point Depth was only achieved using the Fractal based approach. The depth and temperature results from the application of the same fractal parameter β on data with different window sizes L were found to be comparable and below 10%. Changing the window size did not have a significant effect on depth and temperature values. The application of different values of the fractal parameter β on the same or different window sizes had an effect of increasing the deviation of results from the mean by more than 15%. The use of data windows with different sizes does not have a significant effect on the computed depths and temperatures. Fractal based approach results, showed that the conventional Centroid based approach retained results that were comparable to application of the lower fractal parameter β values of 0 to 1, that represent sedimentary type formations. The fractal-based approach is a better technique for determination of magnetic heat source depths and temperatures. The higher fractal parameter $\beta > 3$ retained depths and temperatures in the Curie point range that were indicative of rock formations with an igneous bias.

Acknowledgments

This research project was made possible through funding from Water Research Commission (WRC) K5/1959; National Research Foundation (NRF) Grant UID 82443; Council for Geoscience, South Africa projects: ST-2009-1015, ST-2011-1120, & ST-2013-1169. Geosoft Inc. is thanked for providing processing software.

References

Akbar, S., & Fathianpour, N. (2016). Improving the Curie depth estimation through optimizing the spectral block dimensions of the aeromagnetic data in the Sabalan geothermal field. *Journal of Applied Geophysics*, *135,* 281-287. https://doi.org/10.1016/j.jappgeo.2016.10.018

Arnaiz-Rodríguez, M. S., & Orihuela, N. (2013). Curie point depth in Venezuela and the Eastern Caribbean.

Tectonophysics, 590, 38-51. https://doi.org//10.1016/j.tecto.2013.01.004

Bansal, A. R., & Anand, S. P. (2012). Estimation of depth to the bottom of magnetic sources (DBMS) using modified centroid method from Aeromagnetic data of Central India. *In Proc. 9th Biennial International Conference and Exposition on Petroleum Geophysics, Hyderabad, India, P-343*, 4.

Bansal, A. R., Dimri, V. P., Kumar, R., & Anand, S.P. (2016). Curie Depth Estimation from Aeromagnetic for Fractal Distribution of Sources. In Dimri, V. P. (Ed), *Fractal Solutions for Understanding Complex Systems in Earth Sciences* (pp. 19-31), Springer International Publishing. https://doi.org/10.1007/978-3-319-24675-8

Bansal, A. R., Gabriel, G., Dimri, V. P., & Krawczyk, C. M. (2011). Estimation of depth to the bottom of magnetic sources by a modified centroid method for fractal distribution of sources: An application to aeromagnetic data in Germany. *l*, *76*(3), 11-22. https://doi.org/10.1190/1.3560017

Barker OB, Brandl G, Callaghan CC, Eriksson PG, van Der Neut M. The Soutpansberg and Waterberg groups and the Blouberg formation. In: Johnson MR, Anhaeusser MR, Thomas CR (eds). *The Geology of South Africa; 2006*. p.301–318.

Bektaş, Ö., Ravat, D., Büyüksaraç, A., Bilim, F., & Ateş, A. (2007). Regional geothermal characterisation of East Anatolia from aeromagnetic, heat flow and gravity data. *Pure and Applied Geophysics*, *164*(5), 975-998. https://doi.org//10.1007/s00024-007-0196-5

Bouligand, C., Glen, J. M., & Blakely, R. J. (2009). Mapping Curie temperature depth in the western United States with a fractal model for crustal magnetization. *Journal of Geophysical Research: Solid Earth*, *114*(B11). https://doi.org/10.1029/2009jb006494

Campbell, S. A., Mielke, P., & Götz, A. E. (2016). Geothermal energy from the Main Karoo Basin? New insights from borehole KWV-1 (Eastern Cape, South Africa). *Geothermal Energy*, *4*(1), 9. https://doi.org//10.1186/s40517-016-0051-y

Eletta, B.E., & Udensi, E.E. (2012). Investigation of the Curie point isotherm from the magnetic fields of eastern sector of central Nigeria. *Geosciences*, *2*(4), pp.101-106. https://doi.org//10.5923/j.geo.20120204.05

Jones, M. Q. W. (1992). Heat flow in South Africa. Handbook 14. *Geol. Surv. S. Afr., Government Printer, Pretoria,* p.174

Jones, M. Q. W. (2017). Anomalous geothermal gradients and heat flow in the Limpopo Province, South Africa: Implications for geothermal energy exploration. *South African Journal of Geology 2017*, *120*(2), 231-240. https://doi.org/10.25131/gssajg.120.2.231

Kasidi, S., & Nur, A. (2013). Spectral Analysis of Magnetic Data over Jalingo and Environs North–Eastern Nigeria. *International Journal of Science and Research*, *2*(2), 447-454.

Khojamli, A., Doulati Ardejani, F., Moradzadeh, A., Nejati Kalateh, A., Roshandel Kahoo, A., & Porkhial, S. (2017). Determining fractal parameter and depth of magnetic sources for Ardabil geothermal area using aeromagnetic data by de-fractal approach. *Journal of Mining and Environment*, *8*(1), 93-101. https://doi.org/10.22044/jme.2015.481

Ledwaba, L. Dingoko, O. Cole, P., & Havenga, M. (2009). Compilation of survey specifications for all the old regional airborne geophysical surveys conducted over South Africa. *Council for Geoscience*, p.40.

Maus, S., Gordon, D., & Fairhead, D. (1997). Curie-temperature depth estimation using a self-similar magnetization model. *Geophysical Journal International*, *129*(1), 163-168. https://doi.org/10.1111/j.1365-246x.1997.tb00945-x

Nwankwo, L. I., Olasehinde, P. I., & Akoshile, C. O. (2009). An attempt to estimate the Curie-point isotherm depths in the Nupe Basin, West Central Nigeria. *Glob J Pure Appl Sci*, *15*(3-4), 427-234. https://doi.org/10.4314/gjpas.v15i3-4.48571

Nyabeze, P. K., & Gwavava, O. (2016). Investigating heat and magnetic source depths in the Soutpansberg Basin, South Africa: exploring the Soutpansberg Basin Geothermal Field. *Geothermal Energy*, *4*(1), 1-20. https://doi.org/10.1186/s40517-016-0050-z

Pilkington, M., & Todoeschuck, J. P. (1993). Fractal magnetization of continental crust. *Geophysical Research Letters*, *20*(7), 627-630. https://doi.org/10.1029/92gl03009

Ravat, D., Pignatelli, A., Nicolosi, I., & Chiappini, M. (2007). A study of spectral methods of estimating the depth to the bottom of magnetic sources from near-surface magnetic anomaly data. *Geophysical Journal*

International, *169*(2), 421-434. https://doi.org//10.1111/j.1365-246X.2007.03305.x

Salem, A., Green, C., Ravat, D., Singh, K. H., East, P., Fairhead, J. D., Mogren, S., & Biegert, E. (2014). Depth to Curie temperature across the central Red Sea from magnetic data using the de-fractal method. *Tectonophysics*, *624*, 75-86. https://doi.org/10.1016/j.tecto.2014.04.027

Shabalala, A., Nyabeze, P. K., Mankayi, Z., & Olivier, J. (2015). An analysis of the groundwater chemistry of thermal springs in the Soutpansberg Basin in South Africa: Recent data. *South African Journal of Geology*, *118*(1), 83-90. https://doi.org//10.2113/gssajg.118.1.87

Telford, W. M., Geldart, L. P., & Sheriff, R. E. (1990). *Applied geophysics* (Vol. 1). Cambridge University Press, p.770.

Tiab, D., & Donaldson, E. C. (2015). Petrophysics: theory and practice of measuring reservoir rock and fluid transport properties. *Gulf professional publishing*, p.918.

Copyrights